Wave resource characterization and co-location with offshore wind in the Irish Sea

Neill, Simon

Renewable Energy

DOI:
10.1016/j.renene.2023.119902

E-pub ahead of print: 24/02/2024

Wave resource characterization and co-location with offshore wind in the Irish Sea

Simon P. Neill[a]

[a]*Bangor University, School of Ocean Sciences, Menai Bridge, LL59 5AB, Anglesey, UK*

Abstract

One barrier affecting progress in the wave energy sector is detailed knowledge of the spatiotemporal distribution of waves in shelf sea regions, including their inter- and intra-annual variability. Here, a recent decade (2012 – 2021) of waves is simulated at high-resolution in the Irish Sea – a region with much offshore energy infrastructure. The spectral wave model SWAN is forced with ERA5 wind fields. There is a strong seasonal cycle in wave height and power. In all months except for July, large waves (significant wave height greater than 5 m) can penetrate into the northern part of the Irish Sea, but the most energetic region is the Celtic Sea, where monthly mean wave power exceeds 30 kW/m in December. In this region, wave power strongly correlates with the North Atlantic Oscillation (NAO) from September to March. To investigate the potential for co-location, i.e. to reduce costs through shared infrastructure, wave and wind power were compared at a leased floating wind site in the Celtic Sea. Over the simulated decade, $r^2 \sim 0.5$, demonstrating modest potential for co-location of wind and wave energy technologies in this part of the Irish Sea – considerably less favourable than other sites in the North Atlantic that experience greater swell.

Keywords: Spectral wave model, Wave energy resource, Climate, Variability, Uncertainty, International Electrotechnical Commission

1. Introduction

Understanding the spatiotemporal distribution of waves in shelf sea regions, including their seasonal and inter-annual variability, is important for a range of applications and sectors. Knowledge of long term trends in waves, for example the frequency and magnitude of extreme events, contributes to our understanding of the impacts and mitigation of climate change [1, 2]. Although tidal currents tend to dominate the transport of shelf sea sediments, particularly in sheltered regions, waves increase bed shear stress, enhancing sediment resuspension and enabling (enhancing) suspended sediment transport by weak (strong) tidal currents [3]. The contribution of waves to sediment dynamics can be used to assist mapping the evolution of sea bed sediment distribution over extended time periods – in some cases over thousands of years [4]. As well as affecting marine ecosystems and biodiversity [5], waves affect many maritime activities such as transport and offshore energy. Further, and the focus of this study, waves can be directly exploited as a form of renewable energy conversion, and hence detailed information about their spatiotemporal distribution, including how wave power varies within and between years, is important for resource assessment and characterization [6, 7].

This study focusses on the Irish Sea – a relatively shallow shelf sea environment between Ireland and Great Britain. The Irish Sea experiences complex wave dynamics that are influenced by a combination of local and large-scale meteorological factors. Waves have played a critical role in shaping the Irish Sea since the Last Glacial Maximum [4], influencing sediment transport, erosion and deposition patterns [8]. The wave climate in the Irish Sea is influenced by a combination of factors, including prevailing wind patterns, storm tracks, and local variations in bathymetry/topography, leading to significant temporal and spatial variability in wave properties across the region. The waves in some regions of the Irish Sea interact with strong tidal currents [9] and large tidal ranges [10], further complicating their spatiotemporal variability.

Wave energy resource characterization, particularly at the early stages of project development, is generally performed using numerical models, validated at discrete points in the model domain against in situ datasets, typically sourced from limited existing wave buoy observations [11]. Since phase resolving models are computationally expensive [12], such model assessments are based on (phase averaged) spectral wave models. Various popular *third generation* spectral wave models, such as WAVEWATCH III, SWAN and WAM, adopt a similar approach [13, 14]; however, one consideration between modelling frameworks is whether the grid is structured or unstructured, with the majority of wave models having both options available. In this study, since there is no focus on any particular region of the domain (as would occur if a proposed wave energy array at a known geographic location was to be investigated), a structured (curvilinear) grid is appropriate, providing approximately consistent resolution throughout the study region. Resource assessments can include the theoretical and/or technical resource, with the latter applied once a technology type (or number of technology options) has been selected. In this study, the focus is on theoretical resource assessment (e.g. in units of available power per metre of wave crest, kW/m), since no past study has provided such an assessment for the Irish Sea. However, the outputs from the model, specifically significant wave height and energy wave period, allow for the subsequent calculation of device specific wave power, applying an available power matrix [15].

While wave energy conversion holds promising potential to displace the combustion of fossil fuels, it faces substantial technological challenges, making wave energy one of the more expensive renewable energy technologies at present [16]. One way to reduce costs is to co-locate wave energy with other maritime industries (e.g. aquaculture; [17]) or offshore energy technologies (e.g. offshore wind; [18]). In addition to reducing the costs for each technology, e.g. by sharing infrastructure, cabling and O&M programmes, the combination of multiple renewable energy conversion resources has the further advantage of providing a more balanced (aggregated) power output, provided there is low correlation between the resources [19]. Whereas such co-location potential has been demonstrated for other combinations of energy technologies that rely on weather such as wind and solar [20], wind and wave are more directly linked, since the wave climate relies on the wind climate. Therefore, weaker correlation between wind and wave is found on sites that are characterized by a substantial swell component, such as Lanzarote in the Atlantic [21] and the west coast of Ireland [19]. Areas such as the relatively enclosed (and hence less swell-dominated) North Sea have less potential for wind/wave co-location [18] since the waves tend to be in phase with the local wind. In this study (Section 4.4) the potential for co-location of wind and wave energy in the Irish Sea is investigated, since part of the region is relatively exposed to the North Atlantic.

In this study, a modelling approach is used to understand the spatiotemporal distribution of wave properties and theoretical wave power throughout the Irish Sea, and the potential for co-location with wind in the most energetic regions. Although various wave models that incorporate the Irish Sea have been developed at various spatial and temporal scales (e.g. [22, 23]), and these models are/were generally suited to their purpose, there are still a few areas that need to be addressed. One product that incorporates the

Irish Sea is the Atlantic-European North West Shelf-Wave Physics Reanalysis dataset[1]. This dataset is based on the WAVEWATCH III model [24], with a model resolution of $1/33 \times 1/74°$ (approximately 1.5 km), forced by ECMWF ERA5 wind fields [25]. Although such a resolution can be useful for many applications, it does not facilitate the investigation of subtle spatial changes in wave climate, for example as required for micro-siting of wave energy convertors [26]. In addition, as few models are developed for the specific purposes of wave energy resource assessment, wave energy period is rarely output as a variable, nor is the full wave spectrum routinely used to calculate wave power. Finally, a recent decade needs to be investigated, improving on studies published over a decade ago that encompass the Irish sea (e.g. [27]). The methodology in this study adheres to the IEC (International Electrotechnical Commission) Technical Specification 62600-101 [11], following a *Class 2* (feasibility) resource assessment. A Class 2 resource assessment is the level of assessment conducted prior to undertaking a design level assessment.

2. Study region – the Irish Sea

The Irish Sea has overall dimensions of around 200×400 km. It connects to the Celtic Sea in the south through St. George's Channel, and to the Malin Sea in the North through the North Channel (Fig. 1a). There are two large islands in the Irish Sea (the Isle of Man and Anglesey) along with numerous smaller islands. There is a deeper channel along the west of the Irish Sea, with shallower regions to the east such as Liverpool Bay. The deepest part of this main channel is 250 m (found in the North Channel), but typical depths are around 100 m. Water depths are generally $20 - 40$ m in the shallower regions to the east.

The Irish Sea experiences some of the largest tidal ranges in the world, with a (mean) spring tidal range of 12 m at Avonmouth in the Severn Estuary. Tidal ranges are also large in Liverpool Bay (e.g. 10 m in Liverpool), but there are also regions in the west (Arklow – near Dublin) where tidal range is close to zero due to the presence of an amphidromic point [28]. Some regions are associated with very strong tidal currents, particularly where the currents flow around islands and headlands. Spring depth-averaged current

[1]`https://doi.org/10.48670/moi-00060`

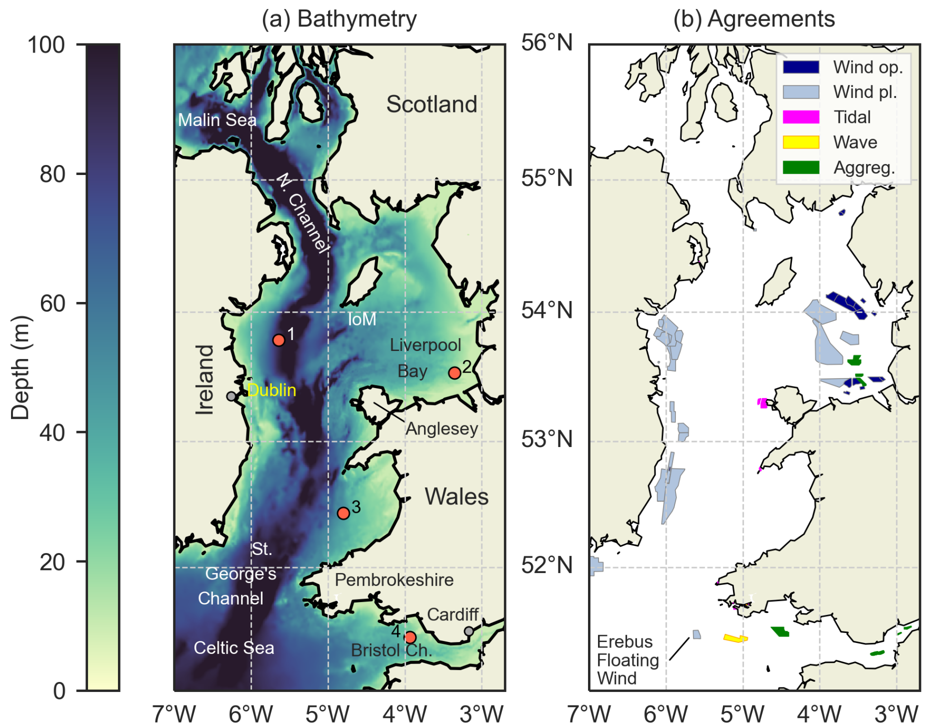

Figure 1: Irish Sea. (a) Bathymtery in metres relative to mean sea level. Red circles are locations of wave buoys used for model validation: 1=AFBI 038A, 2=Liverpool Bay, 3=Cardigan Bay, 4=Scarweather. IoM = Isle of Man. (b) Offshore agreements for wind energy (op. = operational, pl. = planned), tidal stream energy, wave energy, and the extraction of marine aggregates. The location of Erebus Floating Wind Demo is highlighted in (b) as it is used for the co-location analysis presented in Section 4.4.

speeds exceed 2.5 m/s in the Skerries to the northwest of Anglesey [29] and in Ramsey Sound off the coast of Pembrokeshire [30].

The Irish Sea is host to much offshore energy activity including present and future wind farms, planned tidal stream and tidal range projects, and wave energy arrays (Fig.1b). All tidal and wave projects are in the process of development, but 13 wind sites, covering 449 km^2 of seabed, are currently operational. Many additional wind energy sites are at various stages of planning, covering a further 3118 km^2 of sea bed.

3. Methods

The third-generation spectral wave model SWAN (Simulating WAves Nearshore) was used to simulate wave climates over the North Atlantic, and within the Irish Sea. SWAN is an Eulerian formulation of the discrete wave action balance equation [31]. The model is spectrally discrete in frequencies and directions, and the kinematic behaviour of the waves is described by the linear theory of gravity waves. SWAN accounts for wave generation by wind, non-linear wave-wave interactions, whitecapping, and the shallow water effects of bottom friction, refraction, shoaling, and depth-induced wave breaking.

The evolution of the action density ($N = E/\sigma$) is governed by the wave action balance equation which, in spherical coordinates, is

$$\frac{\partial N}{\partial t} + \frac{\partial c_\lambda N}{\partial \lambda} + \frac{\partial c_\phi N}{\partial \phi} + \frac{\partial c_\sigma \ N}{\partial \sigma} + \frac{\partial c_\theta N}{\partial \theta} = \frac{S_{tot}}{\sigma} \tag{1}$$

where E is spectral energy density, σ is angular frequency, θ is wave direction, c_λ and c_ϕ are the propagation velocities in the zonal (λ) and meridional (ϕ) directions, c_σ and c_θ are the propagation velocities in spectral space, and S_{tot} represents the source terms, i.e. generation, dissipation, and non-linear wave-wave interactions.

Version 41.31 of SWAN was run in third-generation mode, with Komen linear wave growth and whitecapping, and quadruplet wave-wave interactions. SWAN default formulations and coefficients were used for all of the physical processes.

3.1. Data

3.1.1. Wind data

Wind data for model forcing was ERA5 – a reanalysis product generated by ECMWF [25]. 10 m components of wind speed (northward and eastward) were extracted 3-hourly over both model domains (outer North Atlantic and inner Irish Sea) at a spatial resolution of $1/4 \times 1/4°$. For the co-location analysis presented in Section 4.4, wind speeds at 100 m height were extracted (to calculate wind power) as this is more consistent with the hub height of wind turbines.

3.1.2. Bathymetry

Bathymetry at both model scales was interpolated to the model grid points from GEBCO, available at a resolution of 15 arc-seconds.

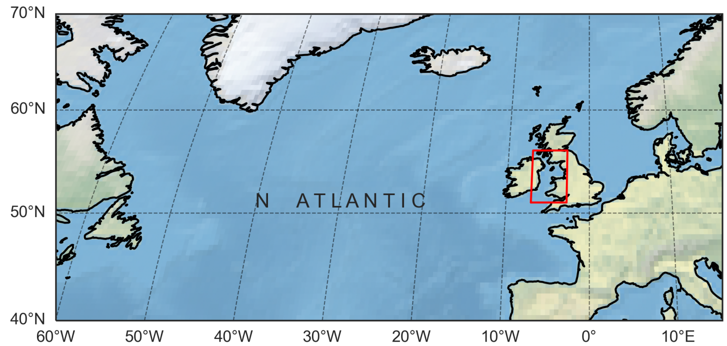

Figure 2: Outer model domain of the North Atlantic wave model. Red box is nested (Irish Sea) region.

3.1.3. Wave buoy data

Wave data used for model validation was extracted from Cefas-Wavenet. The data was hourly, and two different years were used for the validation – 2012 and 2020.

3.2. Outer Atlantic model

Initially, an outer model of the North Atlantic was run, extending from 60°W to 15°E, and 40°N to 70°N (Fig. 2). This model has a spatial resolution of $1/6 \times 1/6°$. Spectral (directional) resolution of this outer model was 8° (i.e. 45 azimuthal directions). Discretized frequencies were in the range $0.04 - 2.0$ Hz, logarithmically distributed into 40 intervals. Three-hourly ERA5 wind fields were used to force this model, which was run for a full decade (2012-2021) at a time step of 15 minutes. Since the Irish Sea is sufficiently far from the boundary (Fig. 2), no boundary conditions were applied to the North Atlantic model. However, two-dimensional action density spectra were output every hour along the boundaries of the Irish Sea nested model at a resolution of $1/12 \times 1/12°$ – a suitable compromise between outer and inner model resolutions.

3.3. Nested Irish Sea model

The nested Irish Sea model extended from 7°W to 2.7°W, and 51°N to 56°N (Fig. 1a). This model was developed on a curvilinear grid, with 516×1011 grid points (i.e. approximately a resolution of $1/120 \times 1/202°$ – a resolution that is consistent with IEC Technical Specification 62600-101 for a Class 2 resource assessment [11]). The Irish Sea grid is described further

Station	Lat	Lon	Year	Useable (%)	R^2	$RMSE$ (m)	$S.I.$ (%)	Bias (m)
AFBI 038A	53°47′.03N	5°38′.20W	2020	100	0.939	0.241	20.44	-0.149
Liverpool Bay	53°32′.00N	3°21′.20W	2012	100	0.930	0.247	29.61	-0.173
Cardigan Bay	52°26′.00N	4°48′.00W	2020	98.8	0.948	0.262	17.46	-0.102
Scarweather	51°26′.00N	3°56′.00W	2012	100	0.884	0.239	20.01	-0.045

Table 1: Details of model validation for H_s. RMSE is the Root Mean Square Error, and S.I. is Scatter Index.

in Lewis et al. [10]. The spectral resolution of this model was identical to the outer model of the North Atlantic. In addition to the boundary forcing from the outer model, the inner nest was also forced by three hourly ERA5 wind fields. The Irish Sea model was again run for a decade (2012 – 2021) at a time step of 2 minutes. Model variables such as significant wave height (H_s), energy wave period (T_e), and wave power (calculated using the full wave spectrum) were output at the model grid points every three hours.

3.4. Validation

The inner nested model was validated at four contrasting locations throughout the Irish Sea (Fig. 1a), using one year of hourly[2] wave buoy data at each location. Two of the locations (Liverpool Bay and Scarweather) were validated throughout 2012, and the other two locations (AFBI 038A and Cardigan Bay) throughout 2020. Agreement between the observations and model are plotted for H_s in Fig. 3, and further details of the validation are provided in Table 1. The validation is an improvement on other, coarser, model studies that incorporate the study region, such as a $1/24 \times 1/24°$ SWAN model of the NW European shelf, forced by ERA-Interim wind fields [27]. For that model, the H_s error metrics calculated for the year 2005 in the middle of the Irish Sea – approximately mid-way between the Cardigan Bay and AFBI 038A wave buoys – were RMSE=0.31 m, Scatter Index (S.I.)=25%, and Bias=-0.16 m.

4. Results

The results focus initially on the fundamental wave properties – H_s, T_e and wave direction – before examining wave power. The results consider both intra- and inter-annual variability.

[2]The hourly wave buoy data were interpolated to the three hourly model output.

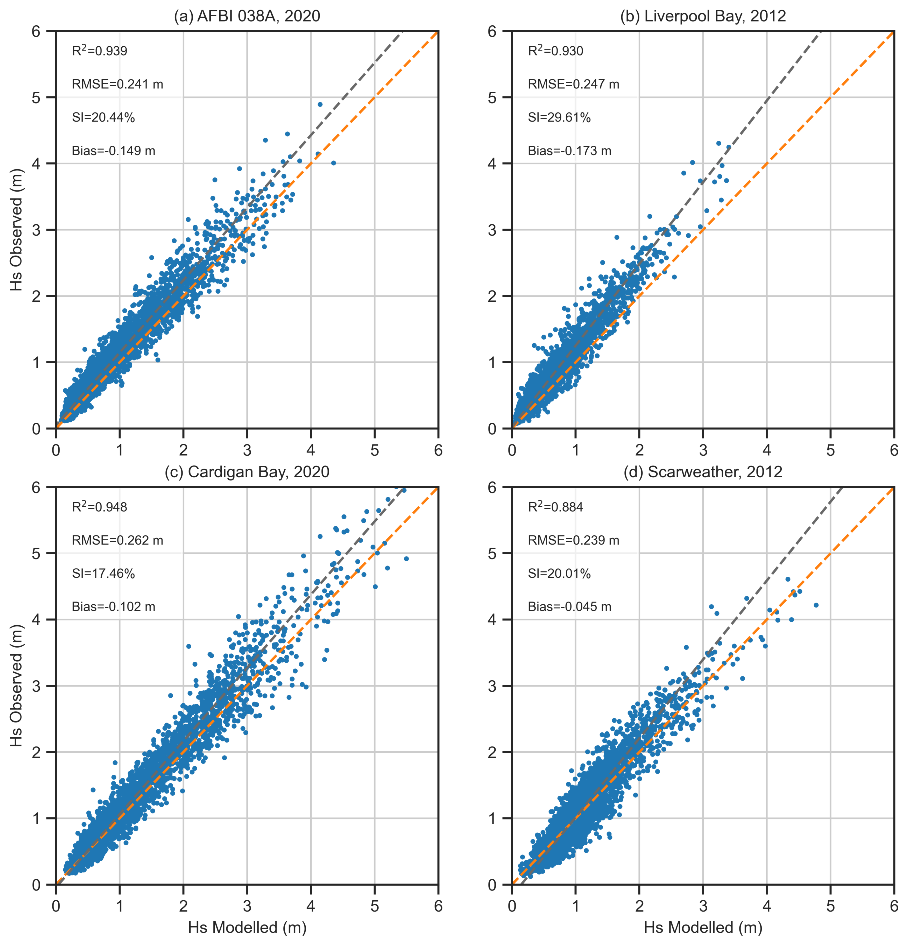

Figure 3: Validation of H_s over one year. Dashed orange line is $x = y$, and dashed grey is line of best fit. Locations of observations shown on Fig. 1a.

4.1. Wave height, period and direction

The spatiotemporal distribution of H_s is shown as an annual cycle of monthly means averaged over all 10 years of simulation (Fig. 4). Given the location of the Irish Sea relative to the North Atlantic, there is a strong seasonal cycle of H_s, with more energetic autumn/winter months (January to March and October-December) compared to spring/summer months. Minimal wave energy propagates into the Irish Sea via the North Channel, but swell waves from the Atlantic penetrate from the south (through St. George's Channel) as far as Anglesey, particularly when supplemented by local winds. The largest wave heights are experienced in the Celtic Sea, where the February mean (for example) H_s is around 3 m. Examining the most energetic year within each month (Fig. 5), it is possible to experience large waves (maximum values of H_s exceeding 5 m) in the northern part of the Irish Sea under certain conditions in all months other than July. Examining February 2014 in more detail, the atmospheric conditions that resulted in this energetic month consist of repeated low pressure systems generated in the Atlantic propagating across the UK (Fig. 6). Peak wind speed during this month was 32.5 m/s or 63 knots (4 February 2014 09:00). Some areas that are persistently sheltered from waves include the north Wales coast and the Severn Estuary (i.e. upstream of the Bristol Channel) – Fig. 5. To compare with a previous WAM modelling study that ecompasses the Irish Sea, the maximum value of H_s simulated by a WAM model in Liverpool Bay from 1996 – 2006 was 5.63 m (1997) [32] – comparable to the maximum values in this region calculated in the current study (Fig. 5).

Energy wave period generally follows the distribution of wave heights (Fig. 7). Longer period (swell waves) are associated with more exposed locations close to the Celtic Sea, where monthly mean wave periods during winter months are around 8 s, reducing to around $5 - 6$ s in the summer. In the northern part of the Irish Sea, average wave periods are typically $4 - 5$ s at all times of the year.

The mean and maximum H_s, T_e and P[3] over the entire decade of simulation are shown in Fig. 8. In the Celtic Sea, the maximum wave height and period are around 10 m and 16 s, respectively. Applying

$$P_{deep} = \frac{\rho g^2}{64\pi} H_s^2 T_e \qquad (2)$$

[3]Calculated using the full wave energy spectrum – see Section 4.2.

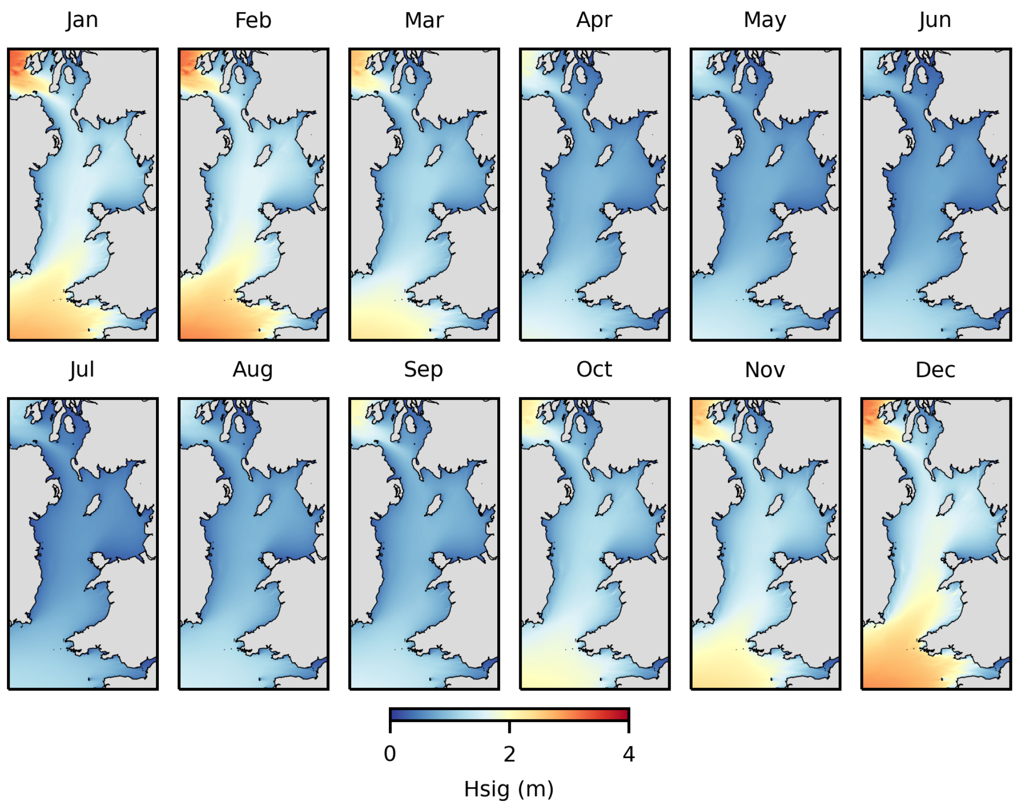

Figure 4: Annual cycle of monthly mean significant wave height averaged over all 10 years (climatological monthly wave height).

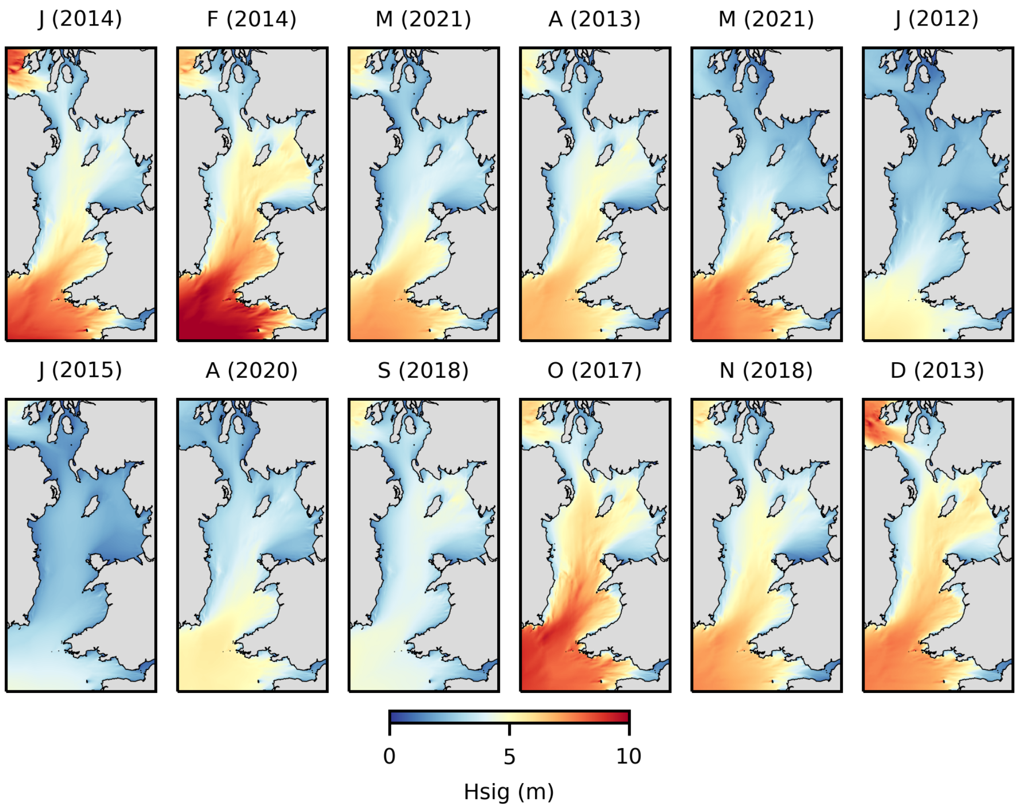

Figure 5: Most energetic years for each month of the year plotted as Hsig. For each month, the most energetic year is given in brackets.

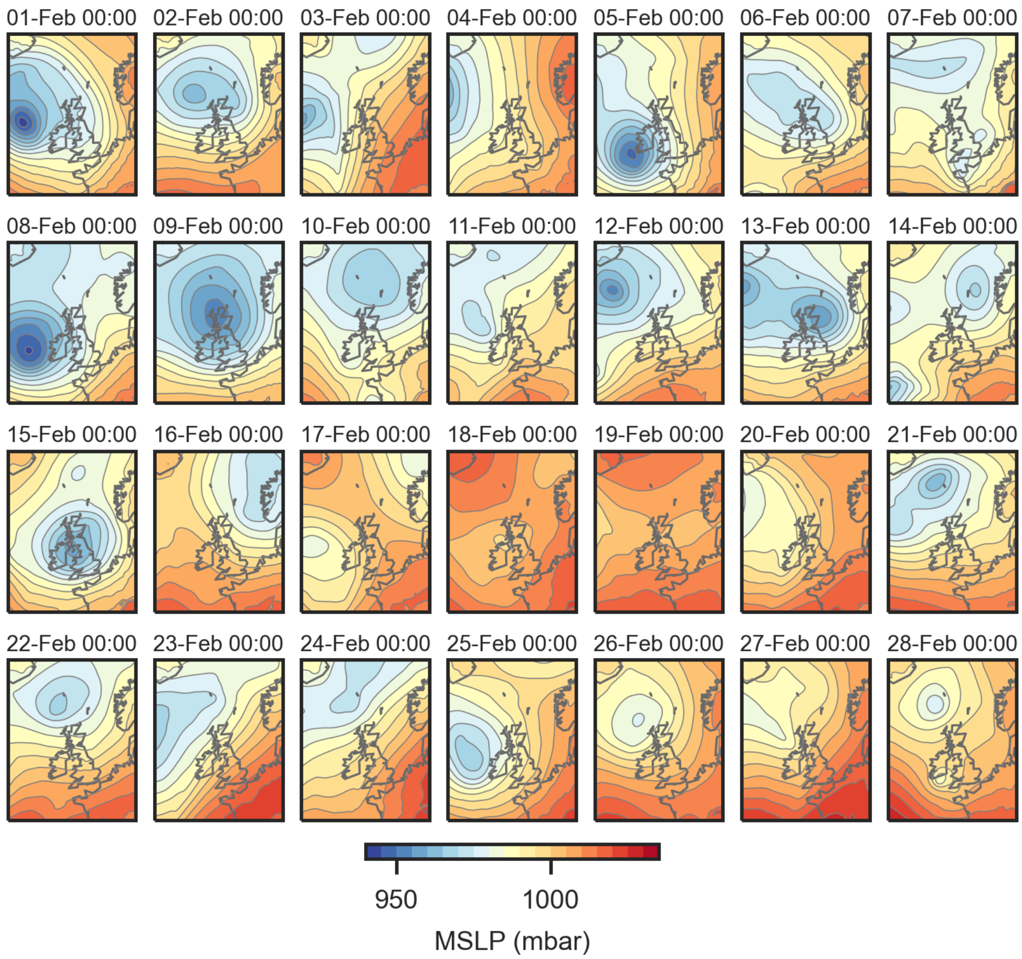

Figure 6: Isobars of mean sea level pressure (in mbar) every 24 hours throughout February 2014 – the month with the largest wave heights over the simulated decade (Fig. 5).

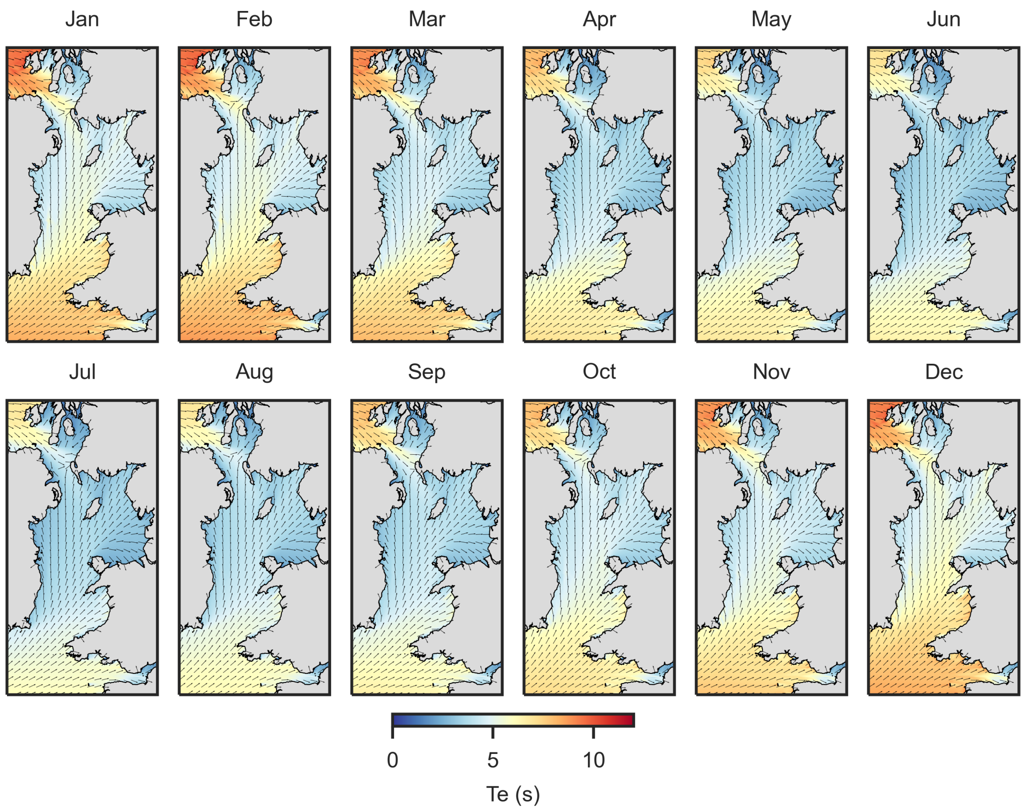

Figure 7: Annual cycle of monthly mean energy wave period (T_e) and wave direction (shown as unit vectors based on the direction of mean energy transport).

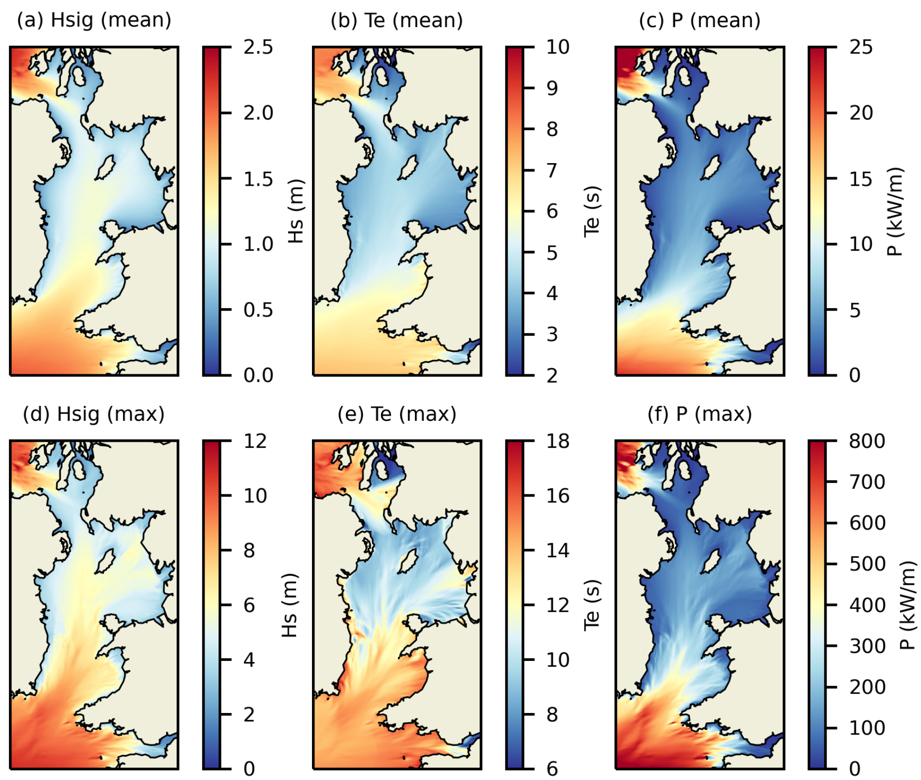

Figure 8: Distribution of mean and peak H_s, T_e and P over the entire decade of simulation. P is directly output from the SWAN model, based on the full wave energy spectrum.

gives a wave power of around 800 kW/m, i.e. corresponding to the peak value in panel (f). Wave power is examined in more detail in the following sections.

4.2. Wave power

The components of wave power (i.e. wave energy flux) were evaluated internally by SWAN, using

$$P_\lambda = \rho g \int \int c_\lambda E(\sigma, \theta) d\sigma d\theta \tag{3}$$

and

$$P_\phi = \rho g \int \int c_\phi E(\sigma, \theta) d\sigma d\theta \tag{4}$$

The annual cycle of monthly mean wave power (i.e. climatological monthly wave power) is shown in Fig. 9. The distribution has much in common with the distribution of H_s, but since wave power is a function of wave height squared (in addition to wave period), the regions of high wave power are more localized, particularly within the Celtic Sea. Again, there is a strong seasonal trend, with January, February and December (i.e. winter months) associated with high wave power. Wave power is minimal from months April to September.

Uncertainty was calculated using

$$\text{uncertainty} = \frac{ts}{\sqrt{n}} \quad (5)$$

where s is the standard deviation, and $t = 1.833$ is Student's t-value at a confidence level of 90% for $n = 10$ samples (i.e. 10 years). Uncertainty in monthly wave power is shown in Fig. 10, focussing only on the six most energetic months (January to March and October to December). The highest uncertainty occurs during February, followed by December. Expressing uncertainty as a percentage of the mean, February stands out, followed by December.

The decadal mean wave power over a large portion of the Irish Sea is relatively low – in the range 5 − 10 kW/m (Fig. 8c). This is similar to the wave energy resource that is found to the east of Orkney (i.e. the region that is sheltered from the North Atlantic) [6] and most of the Mediterranean [33]. The mean winter resource in the majority of the Irish Sea rarely exceeds 20 kW/m (Fig. 10), and so the main part of the Irish Sea is highly unlikely to support wave energy conversion beyond the testing of scaled prototypes. However, in common with previous, albeit coarser, model studies of wave power that encompass the Irish Sea (e.g. [27]), the most energetic region is the Celtic Sea. In this region, the decadal mean wave power is around 20 kW/m (Fig. 8c), with typical winter means of 30−40 kW/m (Fig. 10). These values are comparable to the west coast of Orkney, at the location of the highly successful EMEC (European Marine Energy Centre) grid-connected wave energy test site [34]. It should be noted that instantaneous wave power can exceed 800 kW/m in the Celtic Sea (Fig. 8f), and so devices would require a survivability mode [35].

4.3. North Atlantic Oscillation (NAO)

Many studies have investigated the impacts of natural climate variability on regional or global ocean waves [36]. Key to these studies are climate indices such as the Arctic Oscillation (AO) and North Atlantic Oscillation

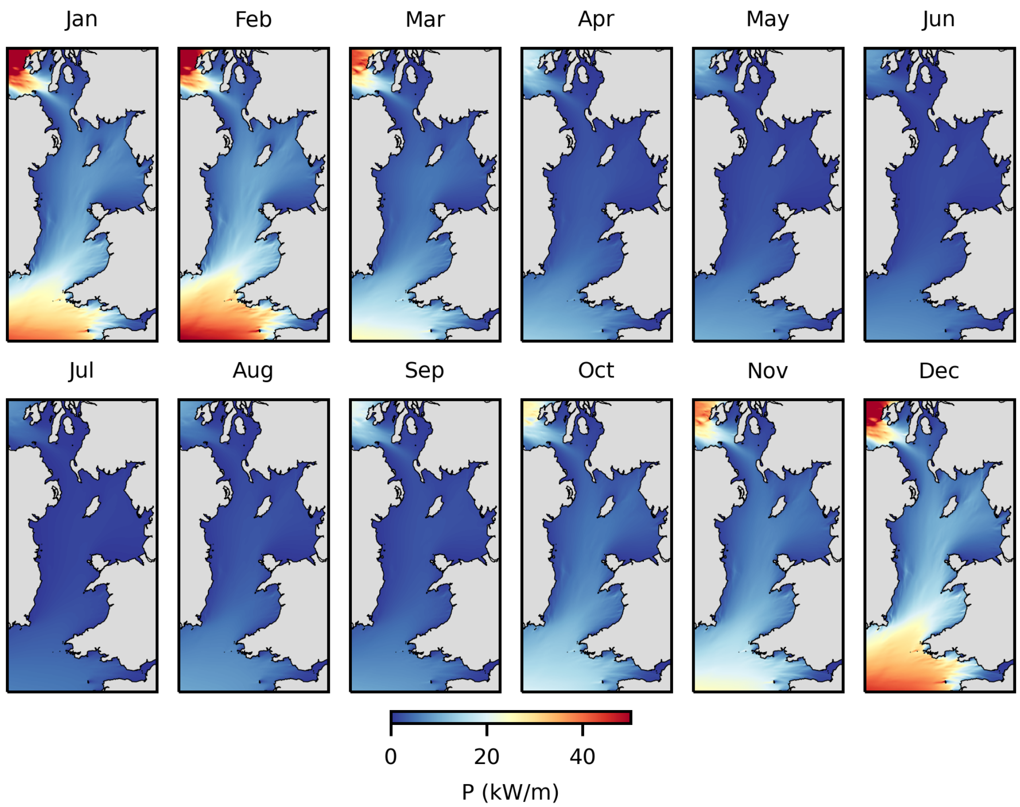

Figure 9: Annual cycle of monthly mean wave power averaged over all 10 years (climatological monthly wave power).

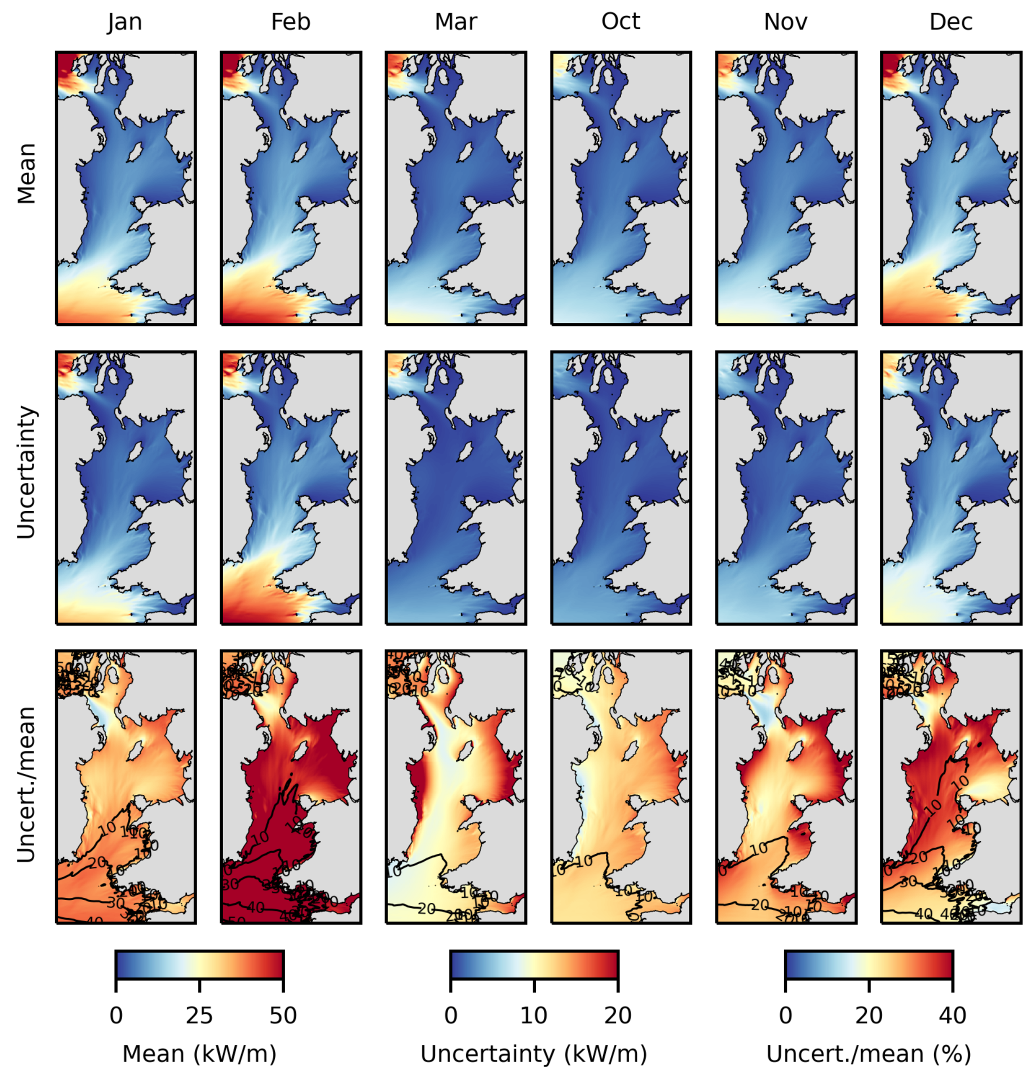

Figure 10: Monthly distribution of mean wave power, wave power uncertainty (90% confidence), and uncertainty expressed as a percentage of mean wave power. Contour values on the bottom panels show mean wave power (i.e. the same data represented in the top row of subplots). Focus is only on the more energetic months (January–March and October–December).

(NAO). The NAO is a climatic phenomenon characterized by fluctuations in atmospheric pressure between the subtropical high over the Azores and the Icelandic Low [37]. The NAO exhibits variability over interannual and decadal timescales. Positive NAO phases are associated with stronger westerly winds and milder winters in northern Europe, while negative phases are associated with weaker westerlies and colder winters. Previous studies have demonstrated that there is a strong correlation between the NAO and wave power in the North Atlantic [38] and in the waters to the north of Scotland [39]. If such a relationship is established for a region or location, this would allow trends in wave power to be explored over long time periods. This relationship is explored here for the most energetic region in the study area – the Celtic Sea.

Wave power was averaged over the region 7°W to 5°W and 51°N to 52°N, capturing the Celtic Sea. Monthly mean wave power over this region was compared against monthly NAO values available from `https://crudata.uea.ac.uk/cru/data/nao/` – an update of the dataset described by Jones et al. [40]. The correlation between NAO and monthly means is shown in Table 2. A threshold of $r \geq 0.5$ was chosen to select only those times of the year when there was a relatively strong relationship between the monthly mean NAO and wave power; therefore only those months where $r \geq 0.5$ are highlighted in bold on the table, corresponding to the period September to March (including the January anomaly where $r = 0.403$). The relationship is not as strong as that reported in the north of Scotland by Mackay et al. – they observed a relatively strong and positive relationship over all months of the year. Here, the continuous period September to March was used to establish a trend between the NAO and monthly mean wave power (Fig. 11). The strength of the relationship over these months is $r = 0.609$ ($r^2 = 0.371$), increasing slightly to $r = 0.623$ ($r^2 = 0.389$) if the January outlier is removed. Therefore, during the months September through to March, higher (positive) NAO values, characterized by stronger westerlies (associated with milder temperatures), results in higher wave power in the Celtic Sea. In contrast, lower (i.e. strongly negative) NAO values are characterized by weaker westerly winds (associated with colder temperatures), and hence reduced wave power in the Celtic Sea.

4.4. Co-location

By developing multiple renewable energy technologies at a single location (co-location) it could be possible to reduce variability in power output and

Month	r
January	0.403
February	**0.670**
March	**0.617**
April	0.355
May	-0.087
June	0.040
July	-0.401
August	-0.128
September	**0.810**
October	**0.674**
November	**0.659**
December	**0.584**

Table 2: Linear Pearson correlation coefficient (r) between monthly NAO and monthly mean wave power averaged over the Celtic Sea (7°W to 5°W and 51°N to 52°N). Those months with $r \geq 0.5$ are highlighted in bold, but note that the continuous autumn-winter-early spring period (September to March) was used for the analysis presented in Fig. 11.

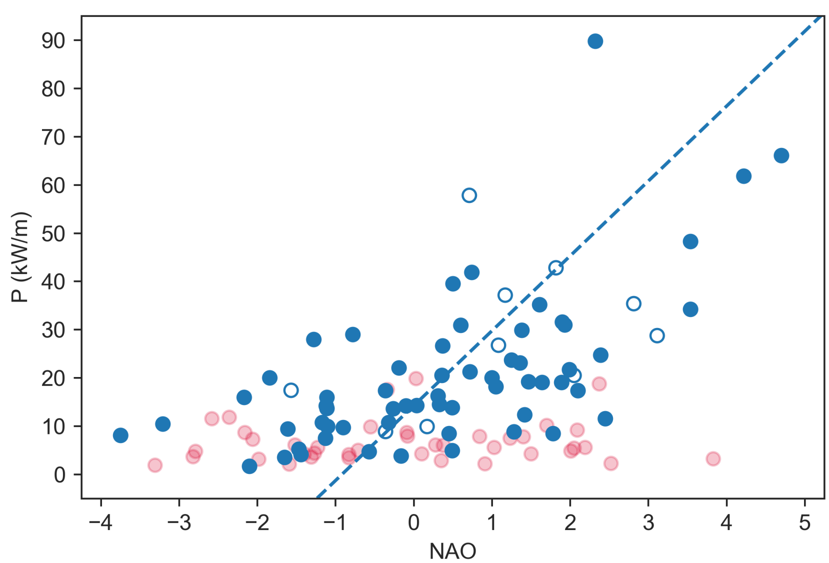

Figure 11: Relationship between monthly NAO index and monthly mean wave power in the Celtic Sea. The dashed trend line ($r^2 = 0.389$) is based on months February, March, September, October, November, December (filled blue circles) and January (open blue circles). Other months are shown as red circles.

reduce overall costs due to shared infrastructure [41]. However, regions are only candidates for co-location if there is a weak correlation between the two (or more) energy resources, otherwise there are no particular benefits in diversifying energy conversion technologies, particularly when one technology (e.g. wave) is considerably more expensive than the other (e.g. offshore wind). Co-location potential was investigated for the most energetic region in the study area – the Celtic Sea.

The primary renewable energy technology in this region is likely to be offshore wind; therefore the detailed wind energy resource was examined at the Erebus Floating Wind Demo site in the Celtic Sea (Fig. 1b) and it was assumed that wave energy technology could at some stage be incorporated into this location. Only theoretical power was considered for both resources – the wave power was based on the full wave spectrum output from the SWAN model (Section 4.2), and the power density of wind was calculated using

$$\frac{P}{A} = \frac{1}{2}\rho U_{100}^3 \tag{6}$$

where A is the swept area of the rotor, ρ is air density, and U_{100} is the instantaneous (3 hourly) wind speed 100 m above sea level (available as a variable directly from ERA5). Variability in power was considered over the entire decade of the wave simulations ($2012 - 2021$). Typical time series (where power is normalized by the maximum over the year) is shown for 2012 (Fig. 12). In this sample time series, there are times when wind and wave are very clearly in phase (e.g. the large events around $3 - 6$ January), and time periods when wind and wave are out of phase (e.g. $26-27$ January). Since both resources are seasonal, correlation coefficients were calculated for each month, capturing all 10 years of simulation over each calendar month (Table 3). The r^2 is relatively consistent across all months, with a mean value of 0.502, but with perhaps more potential for co-location during the months of April ($r^2 = 0.393$) and September ($r^2 = 0.421$). Calculating the cross-correlation (Fig. 13), there is a lag of around 3 hours between wind and wave. Therefore, in the Celtic Sea region, there is moderate potential for co-location between wind and wave – much less so than other regions of the North Atlantic such as Lanzarote (Canary Islands) where the correlation coefficient is consistently low ($r^2 < 0.1$) due to a strong swell component [21].

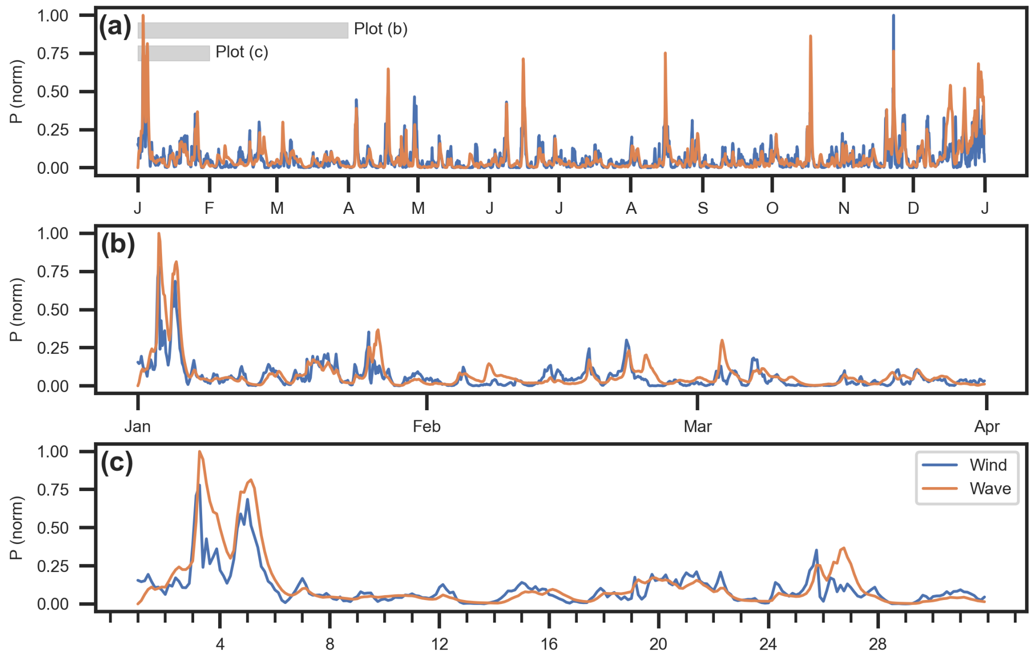

Figure 12: Time series of (normalized) theoretical wind and wave power at the Erebus Floating Wind Demo site in the Celtic Sea during 2012.

Month	r^2
January	0.444
February	0.503
March	0.442
April	0.393
May	0.497
June	0.519
July	0.482
August	0.581
September	0.421
October	0.479
November	0.472
December	0.479
Entire record	0.502

Table 3: Correlation coefficient squared (r^2) between wind and wave power at Erebus Floating Wind Demo during each month (entire 10 year simulation).

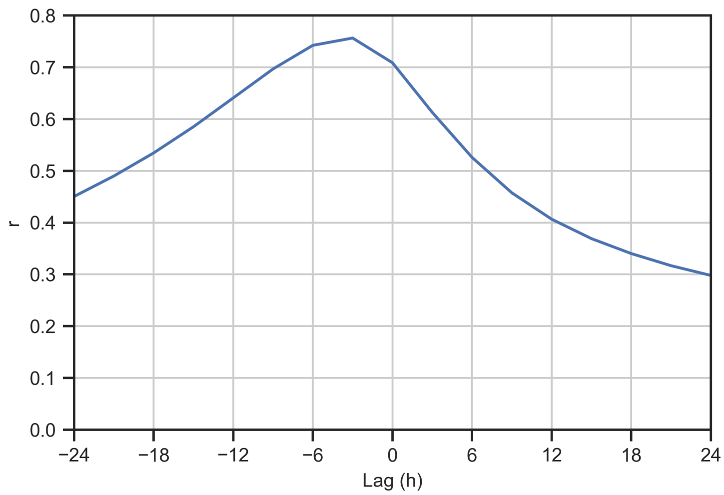

Figure 13: Cross-correlation between wind and wave power at Erebus Floating Wind Demo over the entire 10 year simulation. The maximum correlation was found at −3 h, demonstrating that in general peak wind power leads peak wave power by around 3 h.

5. Conclusions

This model study has provided insights into the spatiotemporal distribution and variability of wave properties and wave power in the Irish Sea, with a particular focus on the energetic Celtic Sea region. The results revealed a distinct seasonal pattern in wave properties, with larger waves and enhanced theoretical wave power during autumn and winter months, attributed to more energetic atmospheric conditions and swell waves propagating from the North Atlantic. The Celtic Sea is the most energetic region in the study area, with a mean December wave power that exceeds 30 kW/m.

The study investigated the relationship between wave power and the North Atlantic Oscillation (NAO), which exhibited a relatively strong correlation during the period September to March. This relationship highlights the potential for using climatic indices like the NAO to predict long-term trends in wave power, facilitating strategic planning for renewable energy applications in regions such as the Celtic Sea.

Examining co-location potential for renewable energy technologies, considering wave and offshore wind, the Celtic Sea demonstrated moderate suitability due to a 3 h lag between wind and wave events. Although the potential for co-location was found to be less promising compared to other regions of the North Atlantic, this finding could be useful for optimizing the renewable energy mix and reducing costs through shared infrastructure.

Although the study is robust, there are a few ways that it could be improved, i.e. possible areas for future work. Although the priority was to simulate a recent decade, extending the analysis to a longer time period (e.g. several decades) would provide an understanding of how wave power in the Irish Sea has changed over time, for example as a result of climate change. The study focussed on the theoretical resource, but extending to the technical resource, particularly in the Celtic Sea, would further help developers converge on a particular technology type. Finally, the (1D and 2D) wave spectra output from the model could be examined in more detail – interesting extensions could be spectral validation against wave buoys, and characterizing bi-modal sea states.

Acknowledgement

I am grateful to the two anonymous reviewers, whose feedback on an earlier version of the manuscript has improved the paper. The wave model simulations were performed on Supercomputing Wales, part-funded by the European Regional Development Fund (ERDF) and administered by the Welsh Government. The author acknowledges the support of the Natural Environment Research Council (NERC) through SWOT-UK project NE/V009109/1.

Data availability

Model bathymetry, wind forcing and validation data are all publicly available from the sources described in the text. The outputs from the wave model are available on reasonable request, noting that the data size is around 1 TB.

References

[1] J.-P. Gattuso, A. K. Magnan, L. Bopp, W. W. Cheung, C. M. Duarte, J. Hinkel, E. Mcleod, F. Micheli, A. Oschlies, P. Williamson, et al., Ocean solutions to address climate change and its effects on marine ecosystems, Frontiers in Marine Science (2018) 337.

[2] J. Morim, M. Hemer, X. L. Wang, N. Cartwright, C. Trenham, A. Semedo, I. Young, L. Bricheno, P. Camus, M. Casas-Prat, et al.,

Robustness and uncertainties in global multivariate wind-wave climate projections, Nature Climate Change 9 (9) (2019) 711–718.

[3] E. V. King, D. C. Conley, G. Masselink, N. Leonardi, R. J. McCarroll, T. Scott, The impact of waves and tides on residual sand transport on a sediment-poor, energetic, and macrotidal continental shelf, Journal of Geophysical Research: Oceans 124 (7) (2019) 4974–5002.

[4] S. P. Neill, J. D. Scourse, G. R. Bigg, K. Uehara, Changes in wave climate over the northwest European shelf seas during the last 12,000 years, Journal of Geophysical Research: Oceans 114 (C6) (2009).

[5] T. Jackson-Bué, A. J. Evans, P. J. Lawrence, P. R. Brooks, S. L. Ward, S. R. Jenkins, P. J. Moore, T. P. Crowe, S. P. Neill, A. J. Davies, Habitat structure shapes temperate reef assemblages across regional environmental gradients, Science of the Total Environment 906 (2024) 167494.

[6] S. P. Neill, M. J. Lewis, M. R. Hashemi, E. Slater, J. Lawrence, S. A. Spall, Inter-annual and inter-seasonal variability of the Orkney wave power resource, Applied Energy 132 (2014) 339–348.

[7] J. Liu, A. Meucci, Q. Liu, A. V. Babanin, D. Ierodiaconou, X. Xu, I. R. Young, A high-resolution wave energy assessment of south-east Australia based on a 40-year hindcast, Renewable Energy (2023) 118943.

[8] S. P. Neill, M. R. Hashemi, A. J. Elliott, An enhanced depth-averaged tidal model for morphological studies in the presence of rotary currents, Continental Shelf Research 27 (1) (2007) 82–102.

[9] M. R. Hashemi, S. P. Neill, P. E. Robins, A. G. Davies, M. J. Lewis, Effect of waves on the tidal energy resource at a planned tidal stream array, Renewable Energy 75 (2015) 626–639.

[10] M. J. Lewis, T. Palmer, R. Hashemi, P. Robins, A. Saulter, J. Brown, H. Lewis, S. Neill, Wave-tide interaction modulates nearshore wave height, Ocean Dynamics 69 (2019) 367–384.

[11] IEC, Technical specification 62600-101: Marine energy – wave, tidal and other water current converters – part 101: Wave energy resource assessment and characterization, Tech. rep., International Electrotechnical Commission (2019).

[12] E. Rusu, C. G. Soares, Modeling waves in open coastal areas and harbors with phase-resolving and phase-averaged models, Journal of Coastal Research 29 (6) (2013) 1309–1325.

[13] J. C. Ortiz-Royero, A. Mercado-Irizarry, An intercomparison of SWAN and WAVEWATCH III models with data from NDBC-NOAA buoys at oceanic scales, Coastal Engineering Journal 50 (01) (2008) 47–73.

[14] J. Monbaliu, R. Padilla-Hernandez, J. C. Hargreaves, J. C. C. Albiach, W. Luo, M. Sclavo, H. Guenther, The spectral wave model, WAM, adapted for applications with high spatial resolution, Coastal Engineering 41 (1-3) (2000) 41–62.

[15] G. J. Dalton, R. Alcorn, T. Lewis, Case study feasibility analysis of the Pelamis wave energy convertor in Ireland, Portugal and North America, Renewable Energy 35 (2) (2010) 443–455.

[16] C. Guo, W. Sheng, D. G. De Silva, G. Aggidis, A review of the levelized cost of wave energy based on a techno-economic model, Energies 16 (5) (2023) 2144.

[17] C. V. Weiss, B. Ondiviela, X. Guinda, F. del Jesus, J. González, R. Guanche, J. A. Juanes, Co-location opportunities for renewable energies and aquaculture facilities in the Canary Archipelago, Ocean & Coastal Management 166 (2018) 62–71.

[18] S. Astariz, G. Iglesias, Selecting optimum locations for co-located wave and wind energy farms. Part I: The Co-Location Feasibility index, Energy Conversion and Management 122 (2016) 589–598.

[19] E. Gaughan, B. Fitzgerald, An assessment of the potential for co-located offshore wind and wave farms in Ireland, Energy 200 (2020) 117526.

[20] P.-Y. Yin, C.-Y. Cheng, H.-M. Chen, T.-H. Wu, Risk-aware optimal planning for a hybrid wind-solar farm, Renewable Energy 157 (2020) 290–302.

[21] D. Christie, S. P. Neill, P. Arnold, Characterising the wave energy resource of Lanzarote, Canary Islands, Renewable Energy 206 (2023) 1198–1211.

[22] S. Pan, Y. Chen, J. Wolf, Y. Du, Modelling of waves in the Irish Sea: effects of oceanic wave and wind forcing, Ocean Dynamics 59 (6, SI) (2009) 827–836.

[23] A. J. Souza, J. M. Brown, J. J. Williams, G. Lymbery, Application of an operational storm coastal impact forecasting system, Journal of Operational Oceanography 6 (1) (2013) 23–26.

[24] H. L. Tolman, the WAVEWATCH III Development Group, User manual and system documentation of WAVEWATCH III TM version 4.18, Technical note, MMAB Contribution 276 (316) (2014).

[25] H. Hersbach, B. Bell, P. Berrisford, S. Hirahara, A. Horányi, J. Muñoz-Sabater, J. Nicolas, C. Peubey, R. Radu, D. Schepers, et al., The ERA5 global reanalysis, Quarterly Journal of the Royal Meteorological Society 146 (730) (2020) 1999–2049.

[26] B. Yang, S. Wu, H. Zhang, B. Liu, H. Shu, J. Shan, Y. Ren, W. Yao, Wave energy converter array layout optimization: A critical and comprehensive overview, Renewable and Sustainable Energy Reviews 167 (2022) 112668.

[27] S. P. Neill, M. R. Hashemi, Wave power variability over the northwest European shelf seas, Applied Energy 106 (2013) 31–46.

[28] H. E. Pelling, J. M. Green, S. L. Ward, Modelling tides and sea-level rise: to flood or not to flood, Ocean Modelling 63 (2013) 21–29.

[29] P. E. Robins, S. P. Neill, M. J. Lewis, Impact of tidal-stream arrays in relation to the natural variability of sedimentary processes, Renewable Energy 72 (2014) 311–321.

[30] I. Fairley, P. Evans, C. Wooldridge, M. Willis, I. Masters, Evaluation of tidal stream resource in a potential array area via direct measurements, Renewable Energy 57 (2013) 70–78.

[31] N. Booij, R. C. Ris, L. H. Holthuijsen, A third-generation wave model for coastal regions: 1. model description and validation, Journal of Geophysical Research: Oceans 104 (C4) (1999) 7649–7666.

[32] J. M. Brown, A. J. Souza, J. Wolf, An 11-year validation of wave-surge modelling in the Irish Sea, using a nested POLCOMS-WAM modelling system, Ocean Modelling 33 (1-2) (2010) 118–128.

[33] L. Liberti, A. Carillo, G. Sannino, Wave energy resource assessment in the Mediterranean, the Italian perspective, Renewable Energy 50 (2013) 938–949.

[34] S. P. Neill, A. Vögler, A. J. Goward-Brown, S. Baston, M. J. Lewis, P. A. Gillibrand, S. Waldman, D. K. Woolf, The wave and tidal resource of Scotland, Renewable Energy 114 (2017) 3–17.

[35] F. Madhi, R. W. Yeung, On survivability of asymmetric wave-energy converters in extreme waves, Renewable Energy 119 (2018) 891–909.

[36] J. Liu, A. Meucci, I. R. Young, A comparison of multiple approaches to study the modulation of ocean waves due to climate variability, Journal of Geophysical Research: Oceans 128 (9) (2023) e2023JC019843.

[37] J. W. Hurrell, Decadal trends in the North Atlantic Oscillation: Regional temperatures and precipitation, Science 269 (5224) (1995) 676–679.

[38] D. K. Woolf, P. Challenor, P. Cotton, Variability and predictability of the North Atlantic wave climate, Journal of Geophysical Research: Oceans 107 (C10) (2002) 9–1.

[39] E. B. Mackay, A. S. Bahaj, P. G. Challenor, Uncertainty in wave energy resource assessment. part 2: Variability and predictability, Renewable Energy 35 (8) (2010) 1809–1819.

[40] P. D. Jones, T. Jónsson, D. Wheeler, Extension to the North Atlantic Oscillation using early instrumental pressure observations from Gibraltar and south-west Iceland, International Journal of Climatology: A Journal of the Royal Meteorological Society 17 (13) (1997) 1433–1450.

[41] S. Astariz, C. Perez-Collazo, J. Abanades, G. Iglesias, Towards the optimal design of a co-located wind-wave farm, Energy 84 (2015) 15–24.